FPS Economy, S.M.E.s, Self-employed and Energy

ECOFLEX

With the support of the Energy Transition Fund

D6.3.2 Design rules of a DC backbone as a function of the available RES, envisaged load infrastructure and flexibility

Version number and Date: Version 1; 19/02/2025
Author (s): Hakim Azaioud (UGENT)

Abstract for dissemination (PU)

This document describes the benefits of integrating Electric Vehicle (EV) chargers into Low-Voltage DC (LVDC) backbones. It begins with an overview of existing literature on this topic, followed by an outline of the modelling approach, which includes behaviour modelling, charging dynamics, and the coordinated EV charging scheme. These models and schemes are then used to evaluate LVDC grids with EV chargers, photovoltaics (PV), and Battery Energy Storage Systems (BESS), and compare them to the benchmark Low-Voltage AC (LVAC) grids.

This document reflects only the views of the author and the Directorate-General for Energy is not liable for any use that may be maybe of the information contained therein

Contents

1. Introduction 4
2. EV Charging on LVDC: A Literature Review 4
3. EV charging modelling 6
3.1 Behaviour modelling 6
3.2 Charging dynamics 7
3.3 Coordinated EV charging scheme 8
4. Grid architecture and specifications 9
4.1 Overview of architectures 9
4.1 On-board charger 9
4.2 Specifications 11
4.3 Assumptions 12
4.4 RELD metric 12
5. Results for opportunistic charging 13
5.1. Correlation between SSI and RELD 13
5.2. Efficiency comparison 14
6. Results for coordinated charging 16
6.1. Self-sufficiency increase 16
6.2 Energy losses 17
7. Conclusion 18
References 22

1. Introduction

Low-voltage DC (LVDC) is an emerging technology in electrical engineering with significant potential to transform energy production, distribution, and utilisation. Previous analyses [1] have demonstrated its benefits in urban areas with high PV penetration, where centralising Battery Energy Storage Systems (BESS) and aggregating Photovoltaic (PV) systems on an LVDC backbone improve energy efficiency and significantly enhance community self-sufficiency. Additional benefits can be achieved by maximising PV utilisation within the LVDC backbone to minimise grid exchanges. Electric vehicles (EVs), which inherently operate on DC, are particularly well-suited for this purpose. However, EV integration also presents challenges such as grid congestion and power quality issues in Low-voltage AC (LVAC) grids [2]. Effectively combining EV demand with PV and BESS is crucial to overcoming these challenges [3], particularly when integrated through an LVDC backbone.

This report presents deliverable D6.3.2, which evaluates LVAC and LVDC architectures for integrating EV chargers in workplace settings using real-world datasets. It also includes a review of existing literature and provides a detailed analysis of loss components and self-sufficiency. In the report of D6.3.1, the historical development of LVDC grids was discussed, covering grid architecture and topologies, the challenge of determining optimal operating voltages, and the development of a dynamic voltage framework. This report builds on that foundation by exploring the benefits of EV charging through an LVDC grid. First, a review of existing literature is presented in **Section 2**. In **Section 3**, the EV charging modelling is discussed, followed by the grid architecture, specifications, and assumptions in **Section 4**. Finally, the results are presented in **Section 5** for opportunistic charging and **Section 6** for coordinated charging, where the impact of the PV-BESS sizing and the number of EV chargers on energetic metrics is studied. This is then followed by the conclusions in **Section 7**.

2. EV Charging on LVDC: A Literature Review

This paragraph provides an overview of existing studies that examine the comparative efficiency between LVAC and LVDC grids, with a focus on EV integration. The article [4] reviewed studies comparing the efficiencies of both grid architectures and proposed a new approach that incorporates multiple parameters, including installed PV capacity, battery State of Charge (SoC), and the specific load and yield power profiles. All of these factors significantly impact efficiency and should be considered in any analysis. However, the authors also pointed out the limitations of many studies, particularly the assumptions made that reduce the quality of the results. While one parameter was held constant, others were varied in discrete steps within a fixed range. Another frequently overlooked aspect is the operating voltage level, which is closely linked to cable and converter losses and their design. The authors conclude with recommendations for future research, particularly on EV integration, which remains an underexplored area. To the best of the author's knowledge, only three articles currently explicitly address the comparative efficiency between LVAC and LVDC systems with EV integration.

The article [5] presents an analysis of energy losses and voltage profiles in LVAC and LVDC grids with EV integration. The authors considered a benchmark radial LV grid topology, with

the capability to switch to a ring-meshed configuration. This grid consisted of several subnetworks, including commercial entities, residential customers, a fast-charging station (FCS), and a mall carpark equipped with EV chargers. Residential customers were assumed to have 2.3 kW or 11 kW chargers, while the FCSs were modeled with powers up to 50 kW. Notably, renewable energy sources (RES) and energy storage solutions were not included in the simulations, and the DC operating voltage level was fixed at 380 V. To generate realistic charging profiles, the authors used driving pattern statistics from New Zealand, applying a stochastic model to simulate the charging behavior. Four EV types, representing the highest market shares in New Zealand, were used, taking into account battery capacity, the nominal power of the on-board chargers (OBC), and the specific energy consumption (energy used per kilometer). The charging powers and types of EVs were randomly assigned to customer nodes. Simulations were conducted over a 24-hour period with a 15-minute resolution. The results indicated that the radial grid configuration resulted in a significant reduction in energy losses, while the meshed configuration led to only marginal differences. Additionally, the minimum voltage in the LVDC grid was found to be 2 to 3 percentage points higher compared to LVAC. However, the study does not provide clarity on whether the energy losses are caused by the converters, cables, or both, nor does it explain how these losses were calculated.

In [6], the application of EV charging on both DC and AC architectures was tested within a workplace environment. The study simulated charging behaviour using fixed arrival times set at 7:45 AM and considered two scenarios involving 10 chargers with capacities of either 11 kW or 22 kW. The DC distribution system also included a PV installation and a BESS; however, the study did not specify the size of the BESS or describe its charging strategy and also did not provide the operating voltage level. Furthermore, the analysis assumed fixed efficiency values derived from commercial converter specifications and literature models, without distinguishing between the efficiencies of AC and DC converters. A typical energy consumption profile of an office building was adopted as the base load profile. Energy losses for both AC and DC architectures were simulated on a daily basis and extrapolated to weekly and yearly levels, meaning that seasonal variations in PV generation were not considered. The results demonstrated that the LVDC architecture, when coupled with a PV system, offered the greatest potential for energy savings due to minimal grid exchanges. The authors recommended further research to investigate various charging scenarios, including cost-benefit analyses, to better understand the implications of these architectures.

The study presented in [7] examined office buildings with EV integration in a unipolar LVDC grid operating at 750 V. The LVDC grid incorporated a PV system, BESS, and multiple EV chargers. The simulation used repetitive daily energy consumption profiles for office buildings, derived from a literature model. Five distinct charging profiles were considered, each with different charging powers, but with fixed behaviour (i.e., consistent arrival and departure times as well as charged energy) over the entire year. A fixed efficiency of 98% for each converter stage and 99% for AC cable efficiency were assumed. The latter was adjusted for DC by multiplying the relative losses by the ratio of theoretical DC/AC cable loss, excluding the power factor on DC and reducing the number of conductors from three to two. The analysis was conducted over a one-year period with a 1-hour resolution. The authors investigated the relative efficiency of DC compared to AC, finding that the efficiency gain was maximal when a high amount of PV generation was coupled with sufficient EV demand, reaching a maximum benefit of 1.5 percentage points. The sensitivity analysis of PV capacity further indicated that when EVs directly consume the produced PV energy, efficiency increases in the DC case, whereas the additional conversion steps in AC lead to higher losses. Including BESS

proved beneficial only when there was sufficient PV capacity, emphasizing the importance of sizing both the PV system and the BESS. **Table 1** presents a comprehensive summary of the applications and limitations associated with the references reviewed.

Table 1. Overview of existing works on comparative efficiency analysis of LVDC and LVAC grids with EV integration

Ref.	Application	Limitations
[5]	Residential and commercial areas	- Simulated one day and excludes hence seasonal variations - Dynamic EV charging behaviour is excluded - No RES and storage excluded - Loss calculation method and efficiencies unspecified
[6]	Workplace charging	- Assumed fixed arrival time and initial SoC - Dynamic EV charging behaviour is excluded - Simulated one day and excludes hence seasonal variations - Fixed efficiency values assumed
[7]	Office buildings	- Simulated with a 1 hour resolution - 5 charging profiles assumed with different but fixed charging powers - Dynamic EV charging behaviour is excluded - Fixed efficiency values are assumed

In addition to the previously mentioned works, other studies have also conducted comparative analyses between LVDC and LVAC grid configurations. The study in [8] explored the economic implications of extending low-voltage distribution networks using either pure DC or hybrid AC/DC systems for the integration of solar PV and EV charging. Conversion losses were calculated using fixed efficiency values, and comparisons were made between traditional AC systems, hybrid AC/DC systems, and pure DC systems. The authors concluded that a parallel pure DC system could be preferable in regions lacking an existing distribution system. A ten-year-old PhD thesis [9] also examined the application of DC and AC grids in buildings with EV, PV, and heat pumps (HPs). While the study did not explicitly investigate energy losses, it focused on other aspects such as grid exchange, peak demand, and voltage imbalances, again using fixed efficiency values for the analysis.

3. EV charging modelling

The modelling of EV charging is comprised of two key parts. The first part focuses on modelling the behaviour of individual users, incorporating the inherent stochastic variations based on available statistical data. This is integrated with a dynamic charging model, which generates current and voltage profiles that reflect the charging process, as controlled by the battery management system.

3.1 Behaviour modelling

The EV charging profiles are stochastically generated based on real-world data collected by ELaadNL, a knowledge and innovation center for smart and sustainable charging of electric

vehicles, initiated by the Dutch grid operators [10]. ELaadNL derived Probability Density Functions (PDFs) for arrival times and initial state of charge $SoC_{ev,init}$ from 10,000 real charging events monitored in 2018 across the Netherlands. These PDFs are categorised into three groups: (i) private customers charging at home, (ii) workplace customers charging at their workplace, and (iii) public customers charging at public locations. The focus of this research is solely on private and workplace charging, with the probability densities used to determine arrival times and the initial SoC of the EVs depicted in **Figure 1**a and b, respectively. It is important to note that workplace chargers are not utilised during the weekend.

3.2 Charging dynamics

A dynamic charging process is applied to avoid overcharging degradation. The charging process consists of a constant current (CC) stage followed by a constant voltage (CV) stage based on the approach presented in [11]. Here, the CV stage reduces the risk of the battery voltage violating its threshold. The obtained dynamic voltage and current charging curves as well as the SoC curve are presented in **Figure 1**c and d. Note that electrical circuit models are usually determined for individual cells, while in this study battery packs consist of multiple cell strings connected in series. Therefore, a conversion is applied. The conversion methodology and parameters used for modelling the dynamic charging process can also be found in [11] and are based on the Nissan Leaf's battery pack.

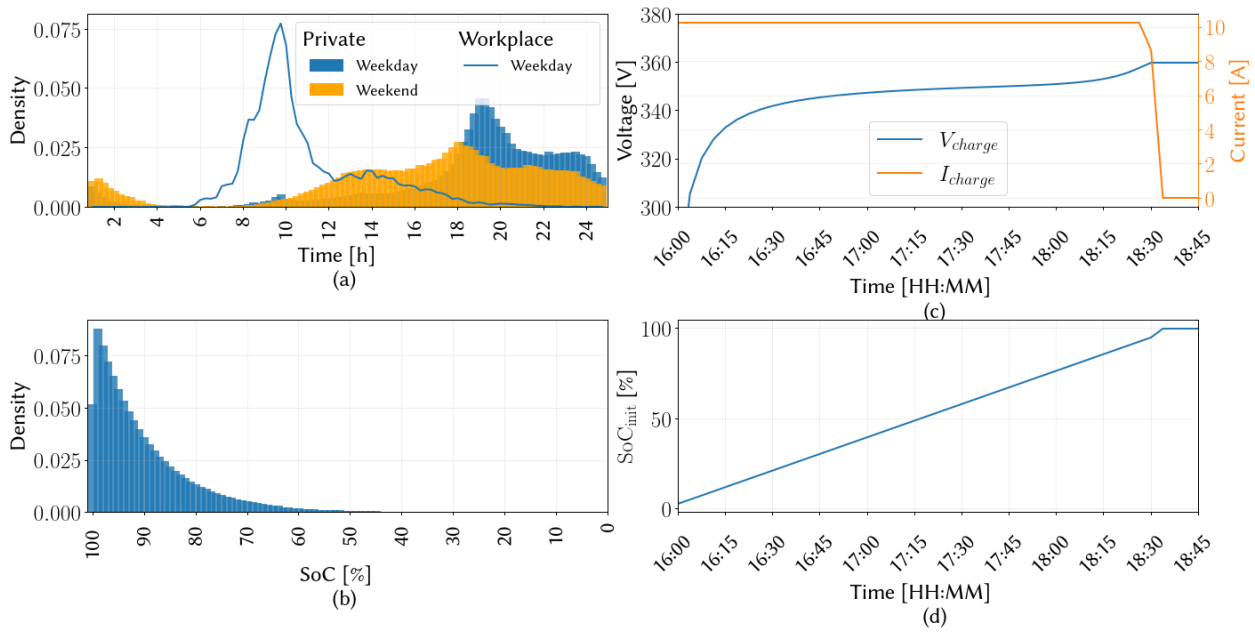

Figure 1. Probability densities and dynamic charging curves, with: (a) the distribution of arrival times for weekdays and weekends; (b) the SoC upon arrival at destination. Both right panels are representative of a randomly selected day with: (c) the charging voltage and current; (d) the $SoC_{ev,init}$ curve

3.3 Coordinated EV charging scheme

This section describes the charging schemes simulated in this study, with a particular focus on the coordinated EV charging scheme. To clearly differentiate the coordinated charging scheme from the opportunistic charging scheme, both are defined as follows:

- **Opportunistic EV Charging:**
    - Charging is uncontrolled, meaning that vehicles start charging immediately upon arrival at the maximum charging rate.
    - Charging stops either upon departure or when the battery reaches a full SoC.
    - This scheme does not consider external parameters, such as the availability of PV generation or the building load.
- **Coordinated EV Charging:**
    - This scheme takes into account the forecasted building load and PV generation.
    - Based on factors such as the targeted SoC and the expected departure time, the EV charging schedule is optimised to achieve specific objectives such as optimising PV utilisation, efficiency, and economic revenues.
    - The optimisation is performed on a day-ahead basis and, in this thesis, assumes an exact forecast of the building demand, PV generation, arrival time, and $SoC_{ev,init}$ of the EV.

In this section, the coordinated charging scheme is exclusively designed to maximise self-sufficiency. However, its formulation inherently incorporates aspects of efficiency. The SSI is computed on a day-ahead basis using 96 samples per day, corresponding to the 15-minute resolution of the demand and PV generation data. The optimisation problem is expressed as a single-objective function, as presented in Equation (1) and (2).

$$\mathrm{SSI} = \frac{\sum_{t=0}^{96} \min(P_{o,\mathrm{pv}}(t) + P_{o,\mathrm{bess},d}(t), P_l(t) + \sum_{i=1}^{n_{\mathrm{ev}}} P_{\mathrm{net,\,ev,\,i}}(t))}{\sum_{t=0}^{96} \left(P_l(t) + \sum_{i=1}^{n_{\mathrm{ev}}} P_{\mathrm{net,\,ev,\,i}}(t)\right)} \tag{1}$$

$$\min f = \mathrm{SSI} \tag{2}$$

The numerator of the SSI quantifies besides the building load P_l the net energy contributions from multiple sources, specifically the net PV generation, the net energy discharged by the BESS, and the net EV demand. These components are mathematically represented as $P_{o,pv}$, $P_{o,bess,ch}$, $P_{o,bess,d}$ and $P_{net,ev,\,i}$. These net energy contributions are calculated using the converter efficiencies. These net energy contributions are calculated using the converter efficiencies. For the PV-BESS system, the efficiency is computed based on converter models described in [12, 1]. The methodology for the EV supply equipment will be detailed later in this report in **Section 4.1**.

The optimisation problem should satisfy following constraints to ensure a feasible operation. The constraints are as follows:

- The EV charging power must remain within its limits, not exceeding the nominal power of the OBC.
- The SoC of the EV must stay within its minimum and maximum bounds to prevent overcharging or over-discharging of the battery.
- The charging time is limited to the period between the EV's arrival and departure times. Outside this time window, the charging power is set to zero.
- The energy required for charging ensures that the EV reaches its desired SoC upon departure or charges as much as possible within the available time window.
- The power balance constraint ensures that the total power supplied by the grid, BESS, and PV equals the total demand.

The optimisation uses the Particle Swarm Optimisation (PSO) algorithm, which is well-suited for the non-convex nature of EV charging optimisation due to its ease of implementation, fewer parameters, and robustness, as noted in [13] and widely applied in the literature [14]. A linearly decreasing inertia weight is applied, ranging from 0.9 to 0.4, to achieve both fast and robust convergence, consistent with the approach in [13]. The cognitive and social weights are both set to 1.5. The optimisation is performed on a day-ahead basis and is repeated for all days of the year, generating n_{ev} timeseries with 35,040 samples each.

4. Grid architecture and specifications

4.1 Overview of architectures

Figure 2 illustrates the grid architectures analysed in this study. In **Figure 2**a, a three-phase LVAC grid integrates three-phase EV chargers, a centralised PV system, and a BESS. Conversely, **Figure 2**b shows the same components connected to an LVDC grid.

4.1 On-board charger

EVs can be charged through various methods, including inductive charging and battery swapping. However, the most widely used method is conductive charging, which can occur using either AC or DC [15]. In AC charging, the EV supply equipment consists of a standard socket that connects the OBC to the LVAC grid. Conversely, DC charging requires an off-board charger as part of the EV supply equipment.

According to the IEC 61815-1 standard, EV charging is classified into four modes based on location and power level, with Mode 4 being the only category that mandates DC charging. Both on-board and off-board chargers use a two-stage AC-to-DC conversion process to charge the battery [16]. Subsequently, the traction power train converts the DC power back into three-phase AC to power the electric motor, as shown in **Figure 3**. This study focuses exclusively on the EV supply equipment.

To mitigate the risk of electric shock, only isolated converter topologies are considered [17]. The conventional full-bridge DC-DC converter is widely used due to its high efficiency and reliability. Additionally, the presence of a transformer allows for a high voltage gain factor.

However, achieving zero-voltage switching across the entire operating range is challenging, especially under light load conditions.

The phase-shifted full-bridge (PSFB) converter, shown in **Figure 4**, addresses this issue by enabling zero-voltage switching throughout the entire operating range, allowing for high-voltage operation with excellent efficiency. This converter uses phase-shift modulation to facilitate the CC and CV charging process, as described in **Paragraph 3.1**. Despite its advantages, the PSFB topology has some drawbacks, including high circulating current during the freewheeling period and significant voltage stress on the rectifier bridge.

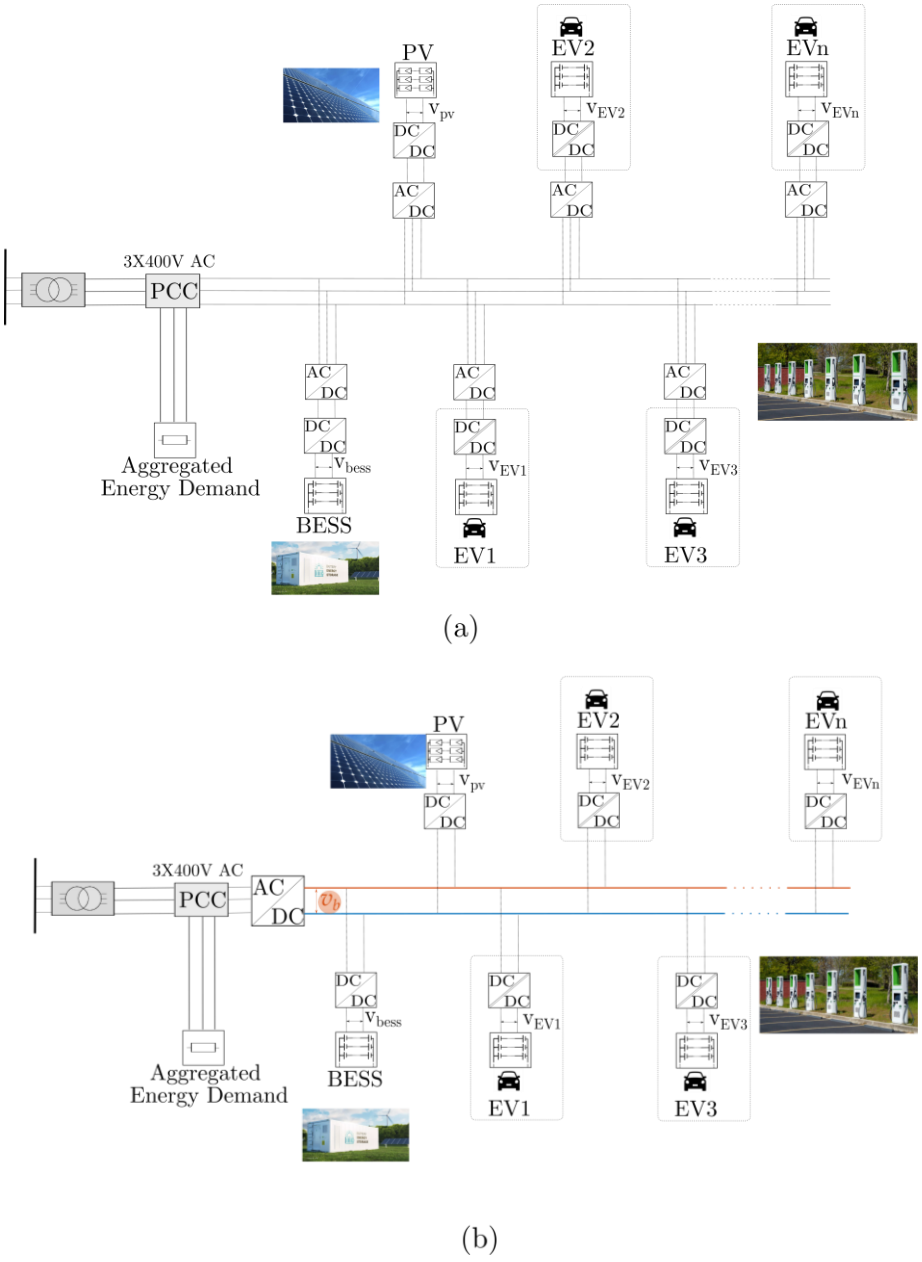

Figure 2. Overview of the grid architectures analysed in this study, with EVs, PV and BESS: (a) LVAC grid architecture, and (b) LVDC grid architecture.

Both on-board and off-board chargers incorporate a DC/AC inverter, employing various inverter topologies. The Vienna rectifier is gaining attention, especially in fast-charging scenarios, due to its high power density and elevated output voltage. It also offers low harmonic distortion, enhancing overall system performance. However, similar to BESS applications, the full-bridge DC/AC inverter and the two-level DC/AC inverter remain the most commonly used topologies in EV supply equipment [18, 19, 20].

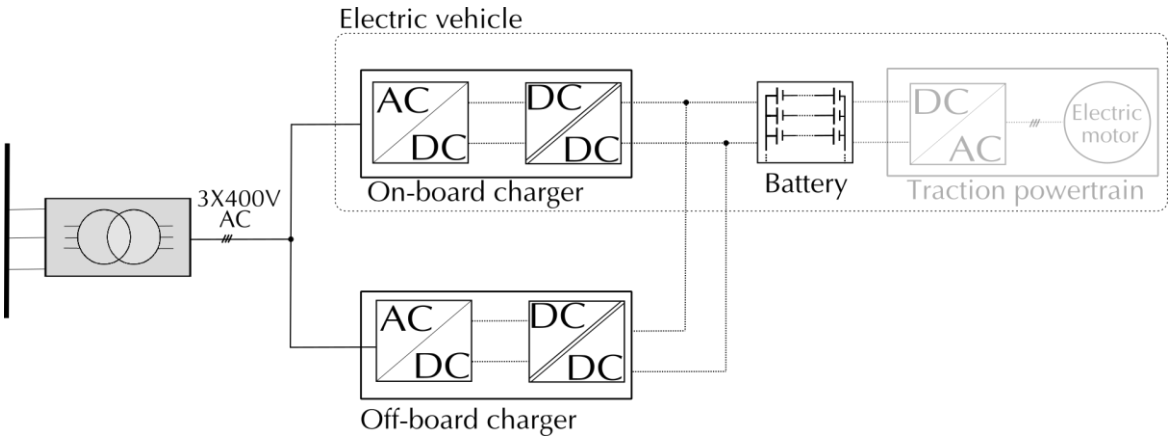

Figure 3. Schematic diagram of the EV supply equipment and powertrain

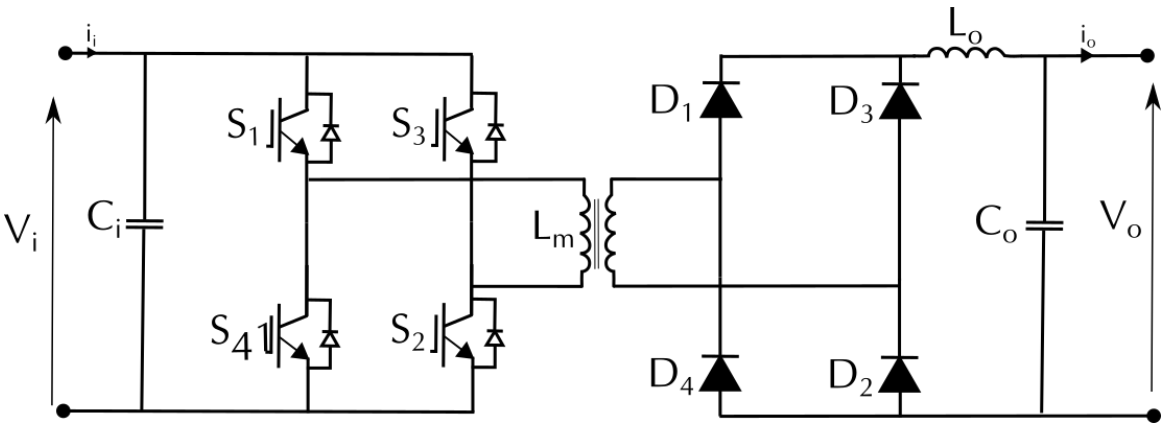

Figure 4. Schematic of the phase-shifted full-bridge converter

The EV DC/DC and DC/AC converters, as well as the central DC/AC inverter and the converters interfacing the PV and BESS, are modeled following the approach outlined in [12, 1, 21].

4.2 Specifications

The analysis considers the following parameters and variables, as summarised in **Table 2**:

- The number of electric vehicles, ranging from 0 to 20.
- Installed PV capacity, varying between 8kW$_p$ and 120kW$_p$.
- Installed BESS capacity, ranging from 8kWh to 120kWh.
- Maximum EV charging power, set at either 11kW or 22kW.

In this study, the annual energy demand is derived from a Small and Medium-sized Enterprise (SME) involved in office-related activities. The load profile for 2021, publicly available from

the Flemish energy regulator [22], is used to represent the energy consumption of the SME. The modelling of the PV-BESS follows the approach outlined in [1, 23].

Table 2. Overview of the simulation variables for the simulations on a residential distribution system with EV, PV, and BESS.

Description	Symbol	Values	Unit
Number of EV chargers	n_{ev}	{1, 2, …, 20}	-
String PV capacity	$P_{unit,\ pv}$	4.14	(kW_p)
Total PV capacity	P_{pv}	$P_{unit,\ pv}$.{2, 6, …, 30}*	(kW_p)
Charging power	P_{ev}	{11, 22}	(kW)
BESS capacity	E_{bess}	$P_{unit,\ pv}$.{2, 6, …, 30}*	(kWh)
Annual building demand	E_{demand}	50	(MWh)

*The unit PV capacity represents a string consisting of 230W modules with 18 modules in series. This value is multiplied by an integer parameter varying from 2 to 26 for sensitivity analysis with BESS size proportional to the PV capacity size.

4.3 Assumptions

For the comparison study applied to workplace EV charging, the following assumptions were made:

- The annual consumption of 50 MWh is assumed for an SME with an office building and 20 employees. This assumption is based on studies [24, 25], which highlight the complexity of accurately modelling consumption profiles. However, these studies show a clear correlation between occupancy rate and consumption. Since the focus of this research is not on consumption details and it impacts efficiency mainly through its effect on BESS utilisation and EV coordination, it is assumed that the consumption, driven primarily by heating, cooling, and ICT, falls within the lower consumption categories identified in the studies referenced.
- The EV charging scheme in this study prioritises the direct utilisation of generated PV energy or stored BESS energy for the EVs, rather than using it for building demand, to minimise conversion losses. However, the coordinated scheme described in **Section 3.3** optimises EV scheduling while considering non-dispatchable building demand. As such, this assumption further confirms that building consumption has a minimal impact on overall energy efficiency.
- Due to the small scale of the cases studied, it is assumed that the cable lengths are minimal enough to result in negligible cable losses, with conversion losses being the dominant factor in the comparative analysis. This assumption also helps reduce computational time, which is important in the context of the stochastic analysis used in this study.

4.4 RELD metric

In addition to the efficiencies and losses, a third metric will also be evaluated. The RELD (Relative Energy Loss Difference) represents the relative difference in losses occurring in a DC grid compared to an AC grid and is shown in (3).

$$RELD = \frac{E_{loss,dc} - E_{loss,ac}}{E_{loss,ac}} \tag{3}$$

5. Results for opportunistic charging

5.1. Correlation between SSI and RELD

The scatter plot in **Figure 5** illustrates the relationship between self-sufficiency, the RELD, instantaneous PV power production, and the number of electric vehicles. A clear correlation is observed between self-sufficiency and RELD, where an increase in self-sufficiency leads to reduced energy imports from the grid, thereby minimising grid exchanges and the power flow through the AC/DC inverter, ultimately reducing its associated losses.

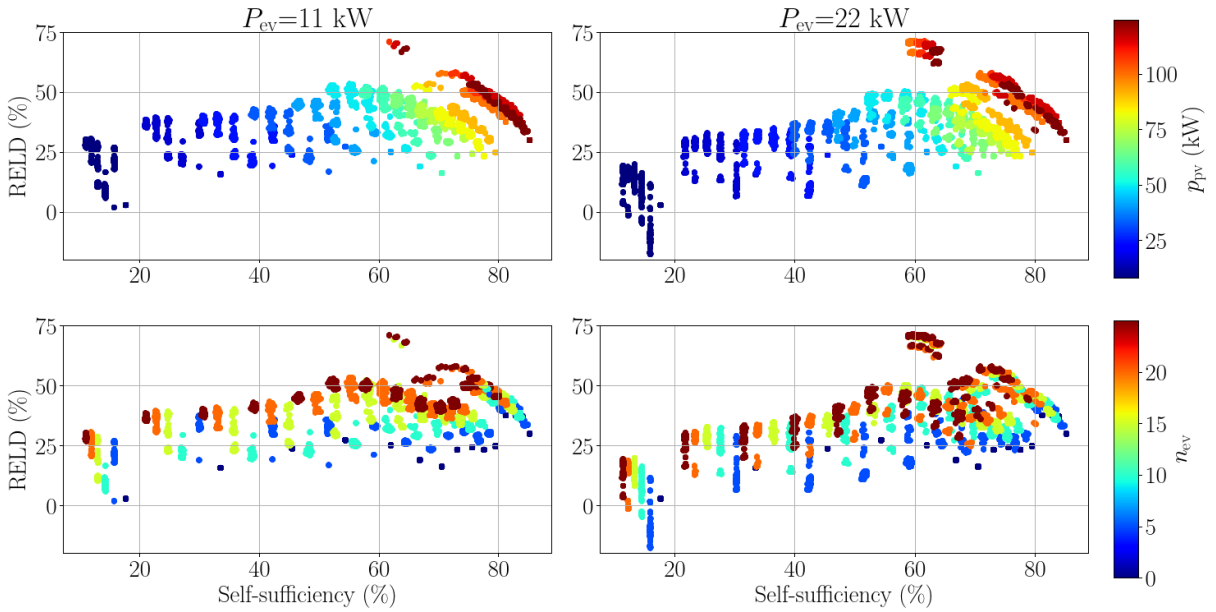

Figure 5. Correlation between RELD and self-sufficiency as a function of instantaneous PV production (upper plots) and the number of EV chargers (lower plots), with 11kW chargers on the right and 22kW chargers on the left.

In the context of the LVAC grid architecture, however, an increase in self-sufficiency leads to higher conversion losses, which in turn favours a higher RELD. The colors in the upper plots demonstrate that as PV power production rises, a larger portion of the EV demand is met by the PV generation, reducing the grid offtake. Conversely, when PV power production is low, the RELD is either lower or negative, particularly when the charging power is set to 22~kW. This suggests that, in these conditions, operating within an LVAC grid architecture results in higher efficiency, primarily due to the sizing of the central DC/AC inverter in the LVDC grid architecture. The inverter is sized based on the highest power exchanged with the grid, which corresponds to the maximum PV power produced in the case with P_{ev}=11 kW, or the maximal aggregated EV power when P_{ev} =22 kW. Thus, during periods of low irradiance, the DC/AC inverter operates within a lower efficiency range, which negatively impacts the conversion loss.

The lower plots exhibit a similar trend, with color variations illustrating the influence of the variable range of n_{ev}, which ranges from 0 to 20. An increase in n_{ev} leads to a higher RELD,

without necessarily improving self-sufficiency. Higher aggregated EV powers result in operation within higher efficiency ranges of the efficiency curve. This plot highlights the synergistic benefits between EVs and PV systems in an LVDC architecture, as it clearly demonstrates higher efficiencies compared to the LVAC grid architecture. When high PV power is accompanied by sufficient EV demand, it leads to higher self-sufficiency, thereby maximizing the benefits of the LVDC architecture.

5.2. Efficiency comparison

To account for the stochastic nature of EV charging behaviour, iterative sampling is employed to generate EV charging demand profiles based on the PDFs presented in **Section 3.1**. The required number of iterations is determined by assessing he convergence of the RELD metric in a preliminary analysis. It was observed that the convergence rate stabilised (with a change of less than 0.1 percentage points) after 75 iterations. When analysing the grid architectures using the iteration methodology and excluding the integration of a BESS, the results in **Figure 6** are obtained. A notable observation is the relatively small variance in RELD values, except in the scenario with 20 EV chargers operating at 22~kW.

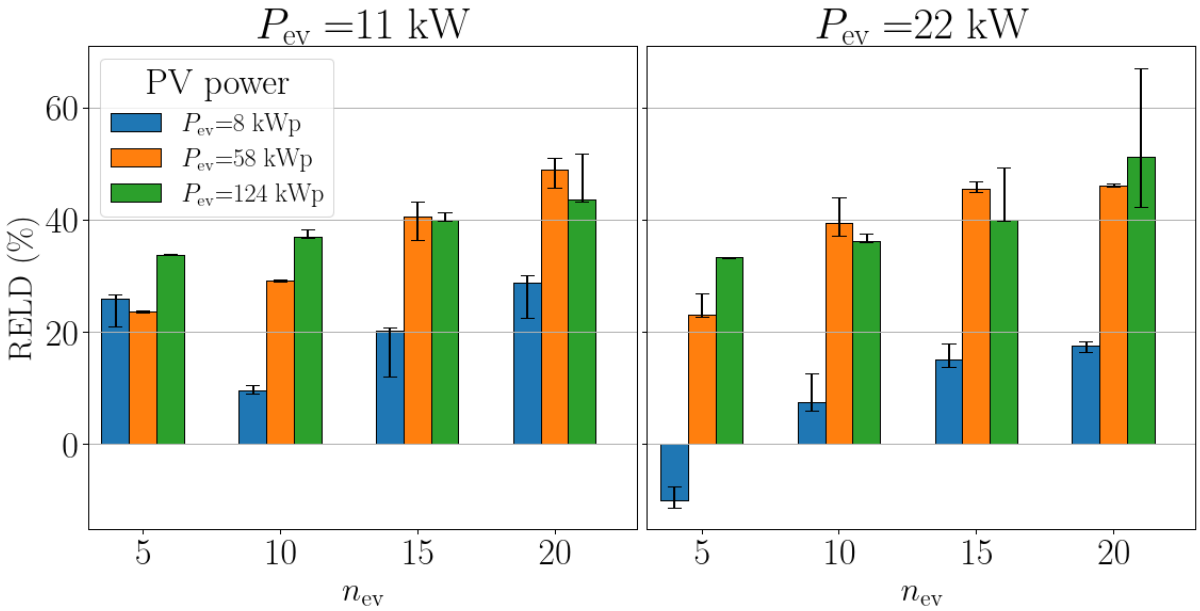

Figure 6. RELD results for 11kW (left) and 22kW (right) EV chargers, shown for three different PV sizes with corresponding interquartile ranges (q25-q75).

This outlier is attributed to the stochastic variability in EV charging profiles, leading to significant fluctuations in the maximum aggregated power and, consequently, variations in DC/AC inverter efficiency. The analysis further highlights the critical importance of asset sizing in determining system efficiency. For instance, with 5 EV chargers at 22 kW and a small PV system, the system exhibits low efficiency, particularly during periods of PV power injection into the grid. This behaviour aligns with the findings discussed in the previous section. Moreover, an increase in the number of EV chargers consistently results in higher RELD values, irrespective of the PV system size. This finding demonstrates that LVDC grid configurations are advantageous even with smaller PV systems, primarily due to scaling effects, as evidenced in [1]. The RELD improvement is particularly pronounced when sufficient PV generation aligns with EV demand, emphasising the importance of appropriately sizing system components to maximise efficiency.

Figure 7 presents a comprehensive analysis of different BESS sizes, confirming previous findings that the greatest benefits are achieved when EV demand is integrated with sufficient PV capacity.

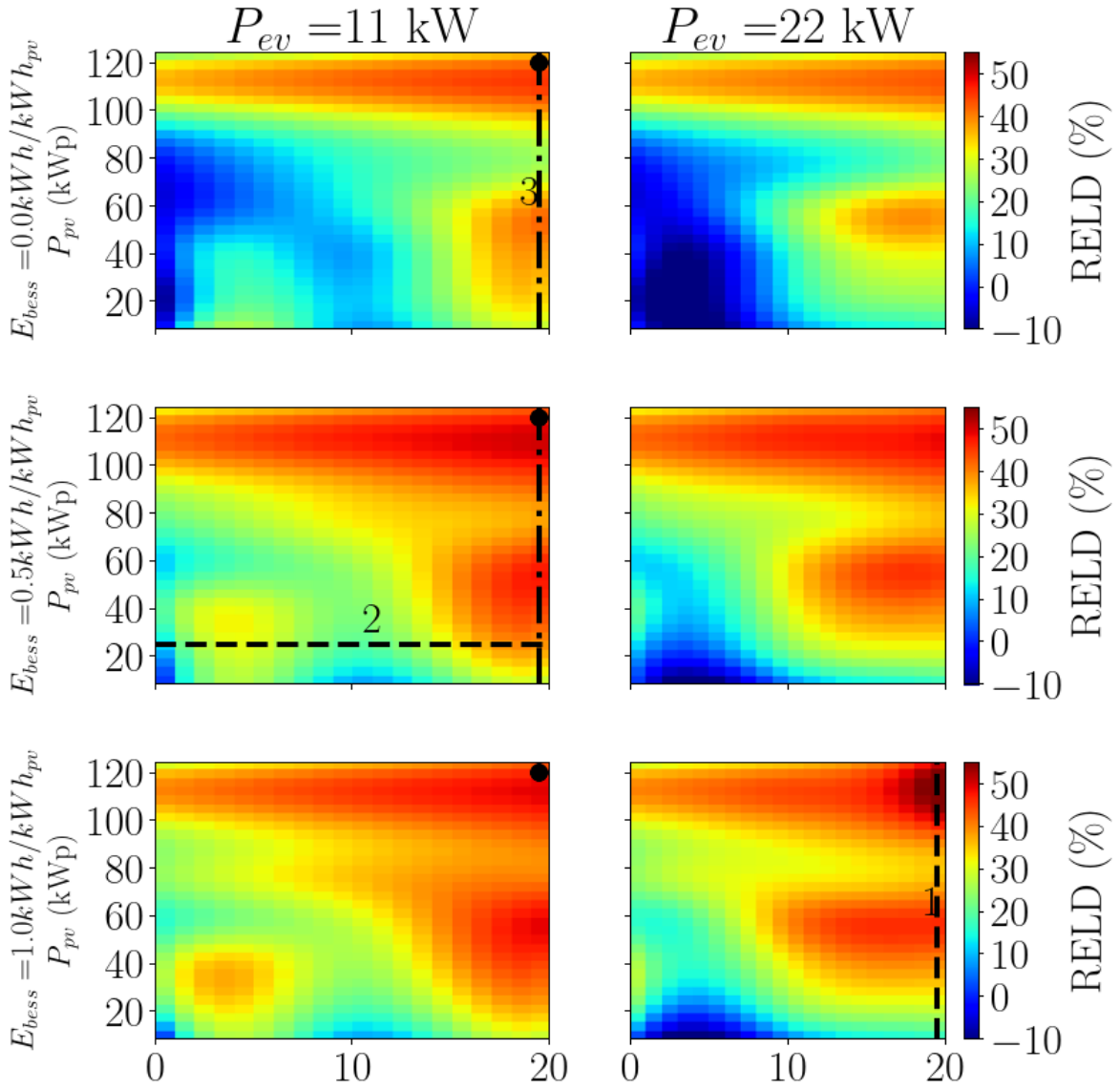

Figure 7. RELD results for 11kW (left) and 22kW (right) EV chargers, presented for three different BESS sizes.

The synergy between EVs and PV systems is evident, as the simultaneous production of PV energy and its consumption by EVs maximises efficiency and energy savings. However, significant gains can also be realised when PV is coupled with BESS in the absence of EVs, especially within an LVDC configuration. These gains are further amplified as the BESS size increases, highlighting the importance of energy storage capacity in optimising system performance. In contrast, when small PV sizes are paired with EV chargers, the RELD remains limited. This limitation arises from the suboptimal efficiency of the central DC/AC inverter, which is sized according to the maximum aggregated EV power. Consequently, the system

operates within a lower efficiency range during PV injection or BESS discharge to meet building demand. This inefficiency is particularly noticeable at 22 kW charging powers.

Moreover, increasing the BESS size enhances the self-sufficiency of the EV demand, thus providing a greater advantage for the LVDC architecture. This highlights the potential of optimising BESS sizing. Further investigations will be conducted to explore the underlying causes of specific trends and discontinuities observed in the results, which will provide deeper insights into the converter efficiency modelling.

6. Results for coordinated charging

6.1. Self-sufficiency increase

As shown in **Figure 8**, the coordinated charging schemes regulates the EV charging demand in a manner that optimises the direct utilisation of available PV generation. In contrast, the opportunistic charging scheme exhibits greater variability, characterised by higher peak power demands that frequently surpass the available PV generation capacity. **Figure 9** illustrates the impact of coordinated charging schemes on the EV self-sufficiency index SSI_{ev}, highlighting a significant increase compared to opportunistic charging schemes.

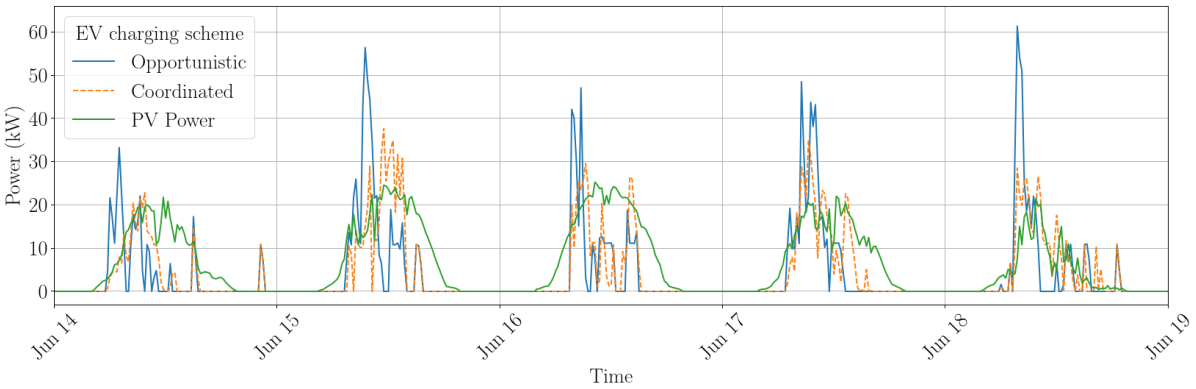

Figure 8. Aggregated EV demand profiles for opportunistic and coordinated charging schemes combined with PV generation. The scenario assumes 20 EV chargers, each rated at 11 kW, and an installed PV capacity of 41 kW.

A larger PV capacity leads to a higher SSI_{ev}, although the increase becomes marginal once the PV output exceeds the EV demand. This point marks the Pareto front, where further scheduling improvements become unfeasible due to the temporal constraints.

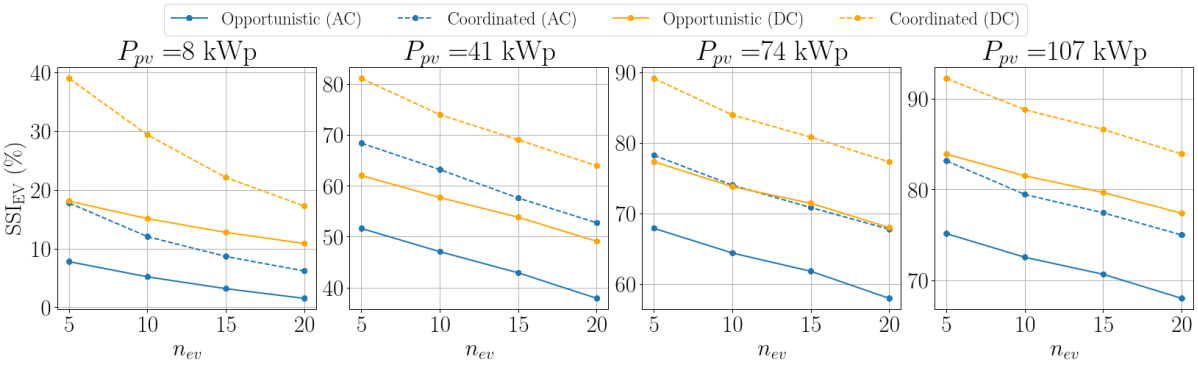

Figure 9. EV self-sufficiency for varying n_{ev} and PV sizes, comparing opportunistic and coordinated charging schemes in LVAC and LVDC architectures with 11 kW chargers.

Notably, the coordinated charging scheme offers a 20 percentage point advantage over the opportunistic charging scheme within the LVDC architecture, particularly for smaller PV sizes. This can be attributed to the fact that a smaller PV system results in a higher direct utilisation of PV production, reducing grid dependence and improving operational efficiency, which in turn increases SSI_{ev}. As the PV capacity grows, this advantage diminishes due to a greater reliance on grid exchanges and lower operational efficiency.

In contrast, when considering the LVAC architecture, the benefit of controlled EV demand is less pronounced, primarily due to higher conversion losses. For a small PV system (8 kW_p), it is more beneficial to use an uncontrolled charging scheme on DC rather than a controlled scheme on AC, underscoring the importance of maintaining high-efficiency operation for maximising SSI_{ev}. Similar trends are observed with 22 kW chargers, as shown in **Figure 10**, though the SSI_{ev} is lower due to the higher charging power.

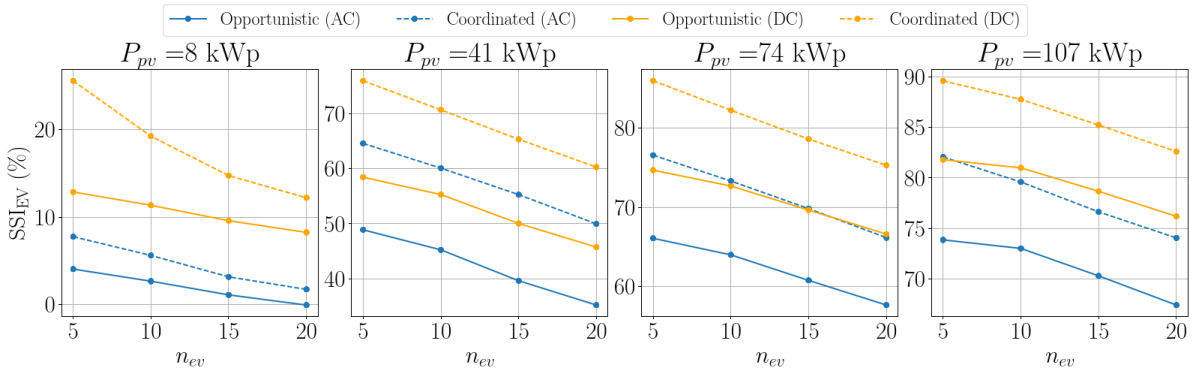

Figure 10. EV self-sufficiency for varying n_{ev} and PV sizes, comparing opportunistic and coordinated charging schemes in LVAC and LVDC architectures with 22 kW chargers.

6.2 Energy losses

The energy loss analysis presented in **Figure 11** clearly demonstrates the superior efficiency of the LVDC architecture across all scenarios. This advantage is mainly attributed to the absence of a double conversion stage in LVDC, in contrast to the LVAC architecture, which incurs higher losses due to the need for two conversions (DC/DC and DC/AC). As the PV size

and number of EV chargers n_{ev} increase, the LVAC architecture experiences a more significant increase in energy losses. Larger PV systems contribute to higher losses in both the DC/DC and DC/AC converters, particularly in the PV and BESS systems. Likewise, increasing the number of EV chargers results in higher losses in the EV-related converters.

The analysis also suggests that the RELD is generally expected to be higher in the coordinated charging scenario. This is due to the increased direct energy consumption by EVs, which amplifies conversion losses in the LVAC architecture. However, the observed RELD is often similar or only marginally higher or lower than in the uncontrolled scenario. This can be explained by the temporal nature of EV charging, which largely takes place during the day and thus already achieves a significant EV self-sufficiency index (SSI_{ev}) in the uncontrolled scenario (**Figure 9**). Additionally, the objective formulation for coordinated charging, detailed in **Section3.3**, accounts for efficiency, ensuring operation in the high-efficiency range of the EV DC/DC and DC/AC converters, which reduces losses.

Another explanation for this behavior lies in the central DC/AC inverter sizing, as discussed in **Section5**. In scenarios with a high number of EV chargers and small PV systems, inefficient operation of the central inverter may occur during PV injection or BESS discharge to meet building demand. In these cases, the coordinated charging scenario benefits from more even distribution of the EV demand over time, preventing such inefficiencies.

As the PV size increases, the losses tend to stabilise across varying values of n_{ev}. In these cases, losses are primarily dominated by the PV system and BESS, with EV-related losses contributing only slightly to the total energy loss.

Similar trends are observed when using 22 kW EV chargers, as shown in **Figure 12**. Higher charging powers lead to more scenarios with elevated RELD in the coordinated charging scheme. This is due to improved utilisation of the PV output, reducing grid import and subsequently lowering energy losses. A noteworthy observation occurs with 20 EV chargers and a PV size of 108 kW_p, where significant energy losses are observed in the opportunistic charging scenario. This increase in loss is linked to the sizing of the central inverter, which is based on the maximum EV demand and exceeds the PV system capacity. However, in the coordinated charging scenario, the distribution of EV demand is more balanced over time, avoiding high synchronous peaks and resulting in lower energy losses.

7. Conclusion

The literature review highlights several challenges associated with integrating EV chargers into LVAC distribution grids. The demand from EVs introduces potential operational issues, including current congestion, which can lead to the overloading of cables and transformers. Voltage-related problems, such as deviations, have also been studied, with voltage unbalance emerging as a critical concern in the case of single-phase EV chargers. A key strategy to address these challenges involves integrating EV chargers with PV systems and implementing control strategies to maximise direct PV consumption, thereby reducing reliance on the grid. This synergy potential could be further enhanced through integration into an LVDC backbone, facilitating simpler and more efficient system operation. However, the literature reveals a significant gap in comparative studies on the efficiency of LVAC and LVDC grids. The few

existing works often suffer from limitations, such as inadequate converter loss modelling, exclusion of dynamic EV charging behaviour, short simulation horizons, or use of unrealistic demand profiles. Furthermore, no studies have been identified that investigate the benefits of coordinated charging in an LVDC architecture.

This report also examined the application of an LVDC architecture in a workplace context, considering both opportunistic and coordinated charging schemes. The key findings of this analysis are as follows:

- An LVDC architecture enhances the EV-PV synergy potential, resulting in more efficient operation and improved PV utilisation. However, when the PV system is undersized and the charging power is increased to 22kW instead of 11kW, the RELD becomes low or even negative. Additionally, it is observed that even in the absence of PV, with only EV chargers connected to the LVDC backbone, the RELD can remain favourable due to the centralised and therefore more efficient DC/AC inverter.
- The relationship between input parameters n_{ev}, PV size, and RELD is non-linear and exhibits certain discontinuities. Further investigation revealed that these discontinuities originate from component parameters, primarily the switching time of the MOSFET, which causes variations in switching losses. Additionally, an analysis of the trends in various component parameters highlights the scaling benefits of centralising .

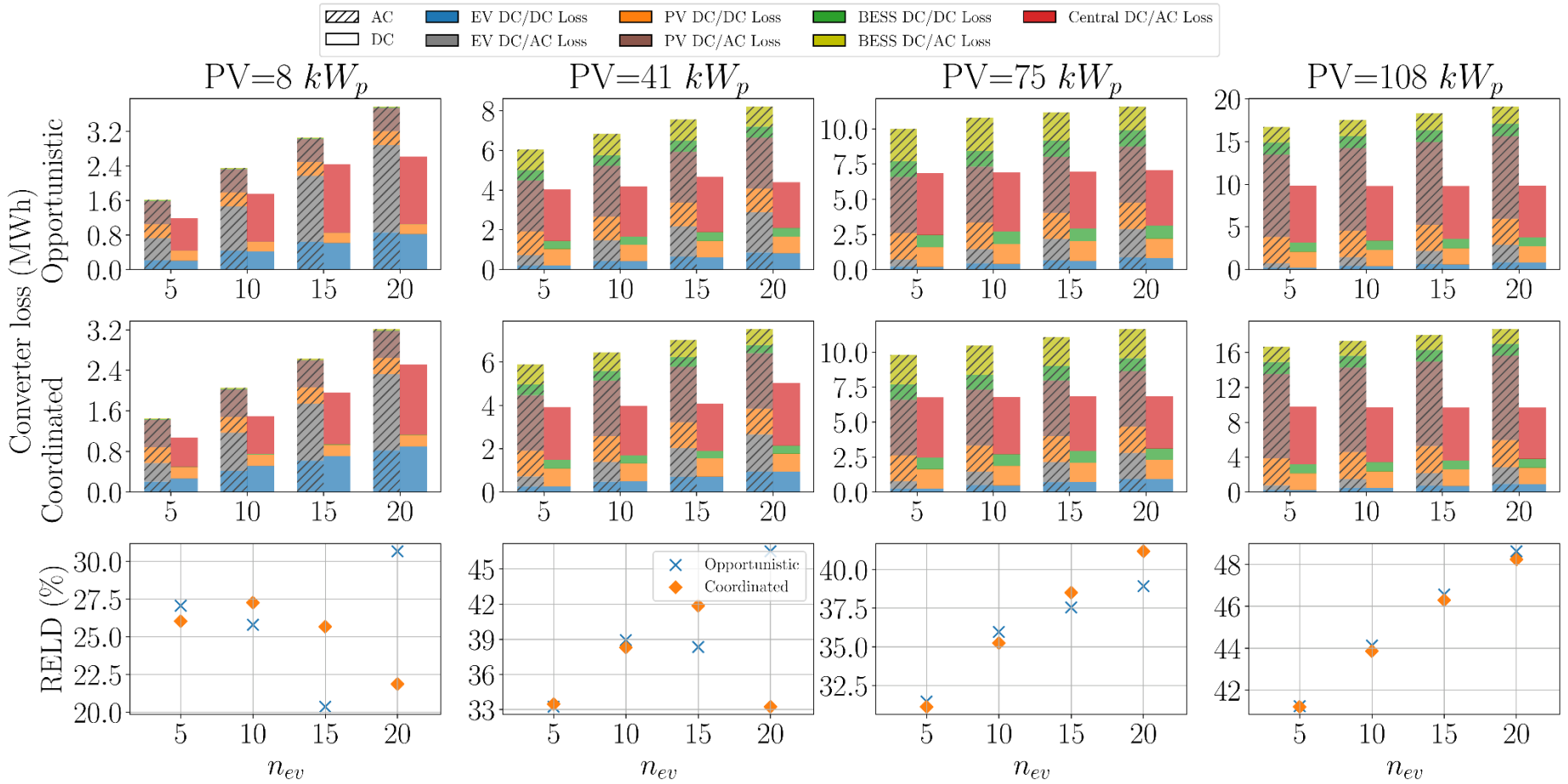

Figure 11. Energy losses for LVDC and LVAC architectures: first row shows opportunistic charging, second row coordinated charging with 11 kW EV chargers, and third row the RELD, all for varying PV sizes.

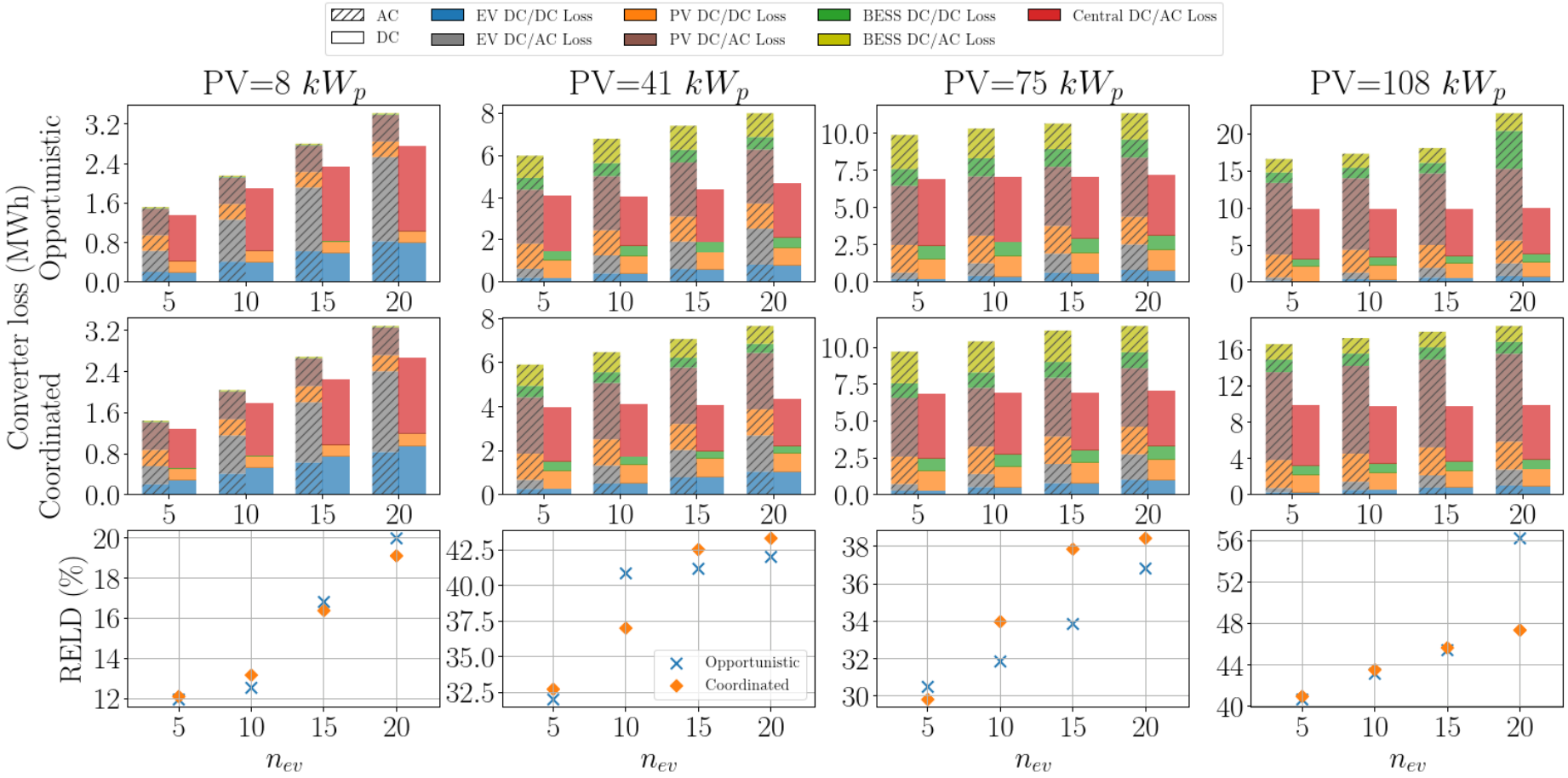

Figure 12. Energy losses for LVDC and LVAC architectures: first row shows opportunistic charging, second row coordinated charging with 22 kW EV chargers, and third row the RELD, all for varying PV sizes.

References

[1] H. Azaioud, R. Claeys, J. Knockaert, L. Vandevelde and J. Desmet, "A Low-Voltage DC Backbone with Aggregated RES and BESS: Benefits Compared to a Traditional Low-Voltage AC System.," *Energies,* vol. 14, 2021.

[2] L. Held, A. Märtz, D. Krohn, J. Wirth, M. Zimmerlin, M. Suriyah, T. Leibfried, P. Jochem and W. Fichtner, "The Influence of Electric Vehicle Charging on Low Voltage Grids with Characteristics Typical for Germany.," *World Electr. Veh. J.* , vol. 10, 2019.

[3] P. Huang, J. Munkhammar and R. e. Fachrizal, "Comparative studies of EV fleet smart charging approaches for demand response in solar-powered building communities," *Sustainable Cities and Society,* vol. 85, 2022.

[4] H. E. Gelani, F. Dastgeer, M. Nasir, S. Khan and J. M. Guerrero, "AC vs. DC Distribution Efficiency: Are We on the Right Path?," *Energies,* vol. 14, 2021.

[5] W. Huynh, T. T. Hoang, A. Ukil and N.-K. C. Nair, "Comparison of Low-Voltage AC and DC Distribution Networks for EV Charging," in *2022 7th IEEE Workshop on the Electronic Grid (eGRID)*, 2022.

[6] M. Yasko, A. Balint, J. Driesen and W. Martinez, "Future workplace EV charging architectures: DC and AC charging choices," in *2023 IEEE International Conference on Electrical Systems for Aircraft, Railway, Ship Propulsion and Road Vehicles & International Transportation Electrification Conference (ESARS-ITEC)*, 2023.

[7] I. Sulaeman, G. R. Chandra Mouli, A. Shekhar and P. Bauer, "Comparison of AC and DC Nanogrid for Office Buildings with EV Charging, PV and Battery Storage," *Energies,* vol. 14, 2021.

[8] S. Jiang, "Extension of low voltage distribution by pure DC or mixed AC/DC parts for integration of solar PV and EV charging," 2022.

[9] J. Van Roy, "Electric vehicle charging integration in buildings," 2015.

[10] ELaadNL, *Data Analytics,* 2020.

[11] S. Pelletier, O. Jabali, G. Laporte and M. Veneroni, "Battery degradation and behaviour for electric vehicles: Review and numerical analyses of several models," *Transportation Research Part B: Methodological,* vol. 103, pp. 158-187, 2017.

[12] N. Mohan, T. M. Undeland and W. P. Robbins, Power electronics: converters, applications, and design, John wiley & sons, 2003.

[13] J. Yang, L. He and S. Fu, "An improved PSO-based charging strategy of electric vehicles in electrical distribution grid," *Applied Energy,* vol. 128, pp. 82-92, 2014.

[14] I. Rahman, P. M. Vasant, B. S. M. Singh, M. A. Al-Wadud and N. Adnan, "Review of recent trends in optimization techniques for plug-in hybrid, and electric vehicle charging infrastructures," *Renewable and Sustainable Energy Reviews,* vol. 58, pp. 1039-1047, 2016.

[15] P. Sandhya and G. K. Nisha, "Review of battery charging methods for electric vehicle," in *2022 IEEE International Conference on Signal Processing, Informatics, Communication and Energy Systems (SPICES)*, 2022.

[16] IEC Technical Committee 69, *IEC 61851-1 Electric Vehicle Conductive Charging System - Part 1: General Requirements,* Geneva, Switzerland: International Electrotechnical Commission (IEC), 2017.

[17] P. Van den Bossche, A. Mentens and G. Dotreppe, "Electrical safety as key issue in EV charging infrastructure," in *The 35th International Electric Vehicle Symposium & Exhibition*, 2022.

[18] M. Khalid, F. Ahmad, B. K. Panigrahi and L. Al-Fagih, "A comprehensive review on advanced charging topologies and methodologies for electric vehicle battery," *Journal of Energy Storage,* vol. 53, p. 105084, 2022.

[19] G. Rajendran, C. A. Vaithilingam, N. Misron, K. Naidu and M. R. Ahmed, "A comprehensive review on system architecture and international standards for electric vehicle charging stations," *Journal of Energy Storage,* vol. 42, p. 103099, 2021.

[20] R. Islam, S. M. S. H. Rafin and O. A. Mohammed, "Comprehensive Review of Power Electronic Converters in Electric Vehicle Applications," *Forecasting,* vol. 5, p. 22–80, 2023.

[21] X. Cheng, G. Xie and F. Deng, "Modeling of phase-shifted full-bridge ZVS converter based on a new expression of effective duty ratio," *IEEJ Transactions on Electrical and Electronic Engineering,* vol. 11, pp. 185-191, 2016.

[22] VREG, *Verbruiksprofielen en productieprofielen,* 2024.

[23] H. Azaioud, J. Desmet and L. Vandevelde, "Benefit Evaluation of PV Orientation for Individual Residential Consumers.," *Energies* , vol. 13, 2020.

[24] V. A. I. en Ondernemen (VLAIO), "Energiescans in KMO's (2017-2018) EINDRAPPORT, DEEL 1," Brussels, 2018.

[25] J. M. Sipma, A. Kremer and J. Vroom, "Energielabels en het daadwerkelijk energieverbruik van kantoren," 2017.